Mn³⁺ stabilization in complex phosphate–fluoride fluxes and its incorporation into langbeinite framework

Ivan V. Ogorodnyk[a],*, Igor V. Zatovsky[a], Vyacheslav N. Baumer[b], Nikolay S. Slobodyanik[a], Oleg V. Shishkin[b], Igor P. Vorona[c]

[a]*Department of Inorganic Chemistry, Taras Shevchenko National University, Volodymyrska Street 64, Kyiv 01033, Ukraine*
[b]*STC "Institute for Single Crystals", National Academy of Science of Ukraine, Lenina ave. 60, Kharkiv 61001, Ukraine*
[c]*Institute of Semiconductor Physics, National Academy of Science of Ukraine, prospect Nauky 41, Kiev 03028, Ukraine*

Abstract

Two new mixed valence manganese-containing orthophosphates with a langbeinite structure have been obtained from the complex fluoride–phosphate melts using the high-temperature flux technique. $M^{IV}F_4$ and $K_2M^{IV}F_6$ (M^{IV}—Zr, Hf) were used as fluoride and polyvalent metal precursors. Obtained langbeinites were investigated using a single-crystal X-ray diffraction, FTIR-, UV–VIS- and electron paramagnetic resonance (EPR)-spectroscopy. Both compounds crystallize in a cubic system (sp. gr. $P2_13$) with cell parameters $a = 10.2106(12)$ and $10.1896(9)$ Å for $K_{1.96}Mn_{0.57}Zr_{1.43}(PO_4)_3$ and $K_{1.93}Mn_{0.53}Hf_{1.47}(PO_4)_3$, respectively. The rigid langbeinite-like framework is built up from the isolated $[MO_6]$ octahedra and $[PO_4]$ tetrahedra interlinked via oxygen vertices. Potassium cations occupy positions in the large closed cavities of the framework. Statistical distribution of manganese and tetravalent metal over two crystallographic positions in octahedral oxygen environment can be observed. The presence of the mixed valence manganese in the reported phosphates was confirmed using UV–VIS and EPR-spectroscopy.
© 2007 Elsevier Inc. All rights reserved.

1. Introduction

Manganese is one of the elements, which forms compounds in a wide range of the oxidation states. A great number of different manganese phosphates are well known nowadays. Such variety could be explained by the occurrence of different oxidation states and corresponding coordination numbers.

Bivalent manganese forms phosphates in a similar way as other bivalent 3d-metals: $Mn_3(PO_4)_2$ [1], MnP_4O_{11} [2] and other. In this reason, several natural occurring minerals and synthetic compounds which contain mixed metal cationic part were found: $Ni_{1.184}Mn_{0.816}(P_2O_7)$ [3], $NaCs(Mn_{0.35}Cu_{0.65})(P_2O_7)$ [4], $Fe_{4.94}Mn_{2.06}(PO_4)_6$ [5], maricite $NaFe_{0.9}Mn_{0.1}(PO_4)$ [6], natrophilite $Na(Mn_{0.93}Fe_{0.07})(PO_4)$ [7], etc. Another interesting group of the

manganese-containing phosphates are compounds of manganese (III): $MnPO_4$ [8], $Mn(PO_3)_3$ [9], $MnHP_2O_7$ [10], $KMn_2O(PO_4)(HPO_4)$ [11], $LiMn(PO_4)(OH)$ [12], $M^IMn(HP_3O_{10})$ (M^{II}—K, Rb, Cs) [13–15], $Cs_3M_3^{II}Mn(P_6O_{18})_2$ (M^{II}—Cd, Zn) [16], $Na_7(Mn_5(PO_4)_3F_{13}(H_2O)_3)$ [17]. Threevalent manganese also was found in minerals: purpurite $Mn_{0.65}Fe_{0.35}(PO_4)$ [18], heterosite $Fe_{0.65}Mn_{0.35}(PO_4)$ [19], ferrisicklerite $Li(Mg_{0.5}Mn_{0.2}Fe_{0.3})_2(PO_4)_2$ [20] and other. Sometimes manganese is mixed-valent in phosphates: $Cs_3Mn_3^{II}Mn^{III}(P_6O_{18})_2$ and $CsMn^{II}Mn^{III}P_6O_{18}$ [21]. Only one phosphate containing manganese (VII) has been reported. $Na_4((Mn_{0.5}P_{0.5})O_4)O$ [22] belongs to the mixed anionic compounds. Both manganese and phosphorus atoms are located in the same position and have tetrahedral oxygen environment.

We report here the synthesis and structural investigations of two new langbeinite-related phosphates containing mixed-valent manganese (II–III) $K_{1.96}Mn_{0.57}Zr_{1.43}(PO_4)_3$ and $K_{1.93}Mn_{0.53}Hf_{1.47}(PO_4)_3$. Both compounds have been

*Corresponding author.
  E-mail address: ogorod@bigmir.net (I.V. Ogorodnyk).

characterized by the FTIR-, UV–VIS- and electron paramagnetic resonance (EPR)-spectroscopy. On the basis of spectroscopic investigations the presence of Mn(II) and Mn(III) was confirmed.

2. Experimental

2.1. Synthesis and identification

Complex fluoride-containing phosphate fluxes indicate high solvent possibilities. Oxides of such polyvalent metals as zirconium, hafnium, chrome and other are low soluble in the pure alkaline phosphate fluxes. The solubility extremely grows in fluoride-containing ones. At the same time fluoride gives a possibility to stabilize unusual oxidation states of different elements (Mn(III), Co(III), etc.).

We used fluoride-containing fluxes in order to obtain zirconium- and hafnium-containing langbeinite-related phosphates. As it was earlier reported [23], such flux can be combined using alkaline phosphates and zirconium fluoride. $K_2M^{IV}F_6$ (M^{IV}—Zr, Hf) was examined as a concurrent fluoride-containing precursor in the flux synthesis. Latter were obtained from $M^{IV}O_2$ using the reported technique [24]. As an initial manganese components were used Mn_2O_3 (extra pure), MnO_2 (pure for analysis) and $Mn(H_2PO_4)_2 \cdot 2H_2O$ (prepared according to [25]).

For optimization of synthetic procedure fluxes with K/P = 1.0–1.35, Zr/P = 0.09–0.15 and Mn/Zr = 1.0–2.0 ranges were examined. In all cases, $M^{IV}F_4$ or $K_2M^{IV}F_6$ and Mn_2O_3, MnO_2 or $Mn(H_2PO_4)_2 \cdot 2H_2O$ were used. Generally, the mixtures of calculated amounts of initial components (without fluorides) were slowly heated up to 1000 °C. At 200, 400 and 800 °C the mixtures were kept for some time to decompose manganese-containing precursors and to evaporate H_2O. In case of using Mn_2O_3 and MnO_2 decomposition was observed at a temperature near 800 °C. At this temperature, the volume of the sintered porous mass extremely grows. At the same time, the mixture melts. So we had some technical difficulties with the mixtures containing Mn_2O_3 and MnO_2. At the temperature, equal to 1000 °C the fluxes were kept during 3 h to evaporate the rest of the decomposition products. On the next stage, the temperature was decreased to 950 °C and fluoride components were added to the flux with stirring using the platinum stirrer. Then the homogenous liquid glass was crystallized in order to obtain the resulting phosphate. The crystallization rate was equal to 25°/h. At a temperature near 600 °C the flux was purred out from the crucible to sheet copper to freeze the crystallization. Finally, the prepared crystals were separated from glass by washing with boiling water. All the operations were performed using the platinum labware.

The optimal ratio of the components were determined as $K_2O \times P_2O_5 \times 0.3K_2M^{IV}F_6 \times 0.3MnO$ which should be better combined using the next components $0.4KPO_3 \times 0.15K_4P_2O_7 \times 0.15K_2M^{IV}F_6 \times 0.15[Mn(H_2PO_4)_2 \cdot 2H_2O]$. According to the noted component ratio 4.0 g KPO_3, 4.2 g

$K_4P_2O_7$ and 3.63 g $Mn(H_2PO_4)_2 \cdot 2H_2O$ were mixed and decomposed as it was reported above. Then 3.6 g K_2ZrF_6 or 4.7 g K_2HfF_6 were added to the flux. As a result crystals with average dimensions near 0.1 mm × 0.1 mm × 0.1 mm were obtained. Green blue crystals had preferably tetrahedral habit.

The purity of the obtained crystals was checked using the powder XRD. The experiment was carried out using a Siemens D500 automated diffractometer (Cu$K\alpha$ radiation, $\lambda = 1.54184$ Å; curved graphite monochromator on the counter arm; step size 0.02°; range 5–90°; scanning rate 10 s/point). Powder pattern indicates high crystallinity for both samples. Obtained crystals are single phased. Chemical composition for both compounds was determined by the energy dispersive X-ray fluorescent spectroscopy using "Elvax light" analyzer. For the crystals, which were used for single crystal X-ray diffraction element ratio was verified by the energy dispersive spectroscopy using a Link Isis analyzer mounted on a Philips XL 30 FEG scanning electron microscope. Element ratio were found to be K: Mn:Zr:P = 1.92:0.6:1.52:3.1 (for $K_{1.96}Mn_{0.57}Zr_{1.43}(PO_4)_3$) and K:Mn:Hf:P = 1.9:0.51:1.54:2.97 (for $K_{1.93}Mn_{0.53}Hf_{1.47}(PO_4)_3$), which are in good agreement with those found using the X-ray fluorescent spectroscopy and calculated on the basis of X-ray diffraction.

2.2. X-ray data collection and crystal data

Structure investigations were performed for well shaped tetrahedral crystals of $K_{1.96}Mn_{0.57}Zr_{1.43}(PO_4)_3$ and $K_{1.93}Mn_{0.53}Hf_{1.47}(PO_4)_3$ colored in green-blue. Experimental diffraction data were collected with an Oxford-Diffraction XCalibur 3 diffractometer equipped with 4 MPixel CCD detectors using monochromated Mo$K\alpha$ radiation ($\lambda = 0.71073$ Å). Space group and cell parameters were determined from all reflections collected over the θ angular range from 2.82° to 30.00°. Multi-scan absorption correction based on symmetry-related measurements was applied to the obtained data [26].

For structure solutions were selected direct method using SHELXS-97 [27]. On three-fold axis were found two potassium atoms and two zirconium atoms. Phosphorus atom was located in general position. The remaining oxygen atoms were found in general positions around the phosphorus atom using the difference Fourier maps. Full-matrix least-square refinement was performed with SHELXL-97 [27]. There were supposed that manganese atoms occupy the same sites as zirconium ones. The atomic coordinates and ADP were constrained for the corresponding Mn and Zr atoms. On the next stage, the occupancies of zirconium, manganese and potassium atoms were refined. The extinction correction was applied for both compounds, but as its value for zirconium phosphate was found negligible comparing with esd it was removed from the final cycles of refinement. Experimental and refinement data is reported in Table 1, and final atomic coordinates and U_{eq} are listed in Table 2.

Table 1
Crystal data and refinement of $K_{1.96}Mn_{0.57}Zr_{1.43}(PO_4)_3$ and $K_{1.93}Mn_{0.53}Hf_{1.47}(PO_4)_3$

	$K_{1.96}Mn_{0.57}Zr_{1.43}(PO_4)_3$	$K_{1.93}Mn_{0.53}Hf_{1.47}(PO_4)_3$
Crystal data		
Crystal system	Cubic	Cubic
Space group	$P2_13$	$P2_13$
Cell parameter (Å)	10.2106(12)	10.1896(9)
V (Å^3)	1064.5(2)	1057.97(16)
Z	4	4
$\rho_{calc.}$ (g/cm^3)	3.265	4.093
Crystal dimensions (mm)	$0.12 \times 0.08 \times 0.05$	$0.1 \times 0.09 \times 0.07$
Data collection		
Measurement device	XCalibur 3 CCD	XCalibur 3 CCD
Wavelength (Å)	0.71073	0.71073
Monochromator	Graphite	Graphite
Scan mode	φ and ω	φ and ω
μ (mm^{-1})	3.356	16.324
Absorption correction	Multi-scan	Multi-scan
T_{min}, T_{max}	0.7532, 0.8273	0.2358, 0.3542
Number of reflections	45023	47553
Independent reflections	1055	1035
Reflections with $l > 2\sigma(I)$	1018	1020
$R_{int.}$	0.0354	0.0404
Theta max. (deg)	29.97	29.96
$h =$, $k =$, $l =$	$-14 \rightarrow 14$; $-14 \rightarrow 14$; $-14 \rightarrow 14$	$-14 \rightarrow 14$; $-14 \rightarrow 14$; $-14 \rightarrow 14$
$F(000)$	998.6	1187.3
Solution and refinement		
Primary solution method	Direct	Direct
Weighting scheme	$w = 1/[\sigma^2(F_o^2) + (0.0293P)^2 + 2.5557P]$ where $P = (F_o^2 + 2F_c^2)/3$	$w = 1/[\sigma^2(F_o^2) + (0.0030P)^2 + 3.6065P]$ where $P = (F_o^2 + 2F_c^2)/3$
$R_1[F^2 > 2\sigma(F^2)]$	0.0298	0.0143
R_1(all)	0.0308	0.0147
wR_2	0.0676	0.0291
S	1.286	1.261
Number of parameters	62	63
Extinction correction	None	SHELXL; 0.00095(12)
$(\Delta\rho)_{max, min}$ (e/Å^3)	0.579, -0.55	0.508, -0.472
Flack parameter	$-0.02(6)$	$-0.020(11)$

2.3. Spectroscopic investigations

The FTIR-spectra were collected at room temperature in KBr disks using Nicolet Nexus FTIR spectrometer at 400–4000 cm^{-1}. The measurements were performed in transmissions mode. UV–VIS-spectra were recorded in the diffuse reflectance mode using SPECORD-40M spectrometer at 12,000–40,000 cm^{-1}. EPR spectra on powdered polycrystalline samples were obtained at X-frequencies (9.438 GHz at room temperature and 9.249 GHz at 77 K) with a "Radiopan" spectrometer.

3. Results and discussion

3.1. Synthetic procedure

The crystallization of langbeinite isotypic phosphates with a general composition $K_2M_{0.5}^{II}Ti_{1.5}(PO_4)_3$, where M^{II}—Mn, Co, Ni, in the fluxes of potassium phosphates containing dissolved titanium and bivalent metal oxides

was reported previously [28,29]. In this reason, we decided to obtain isotypic complex phosphates containing at the same time manganese and zirconium or hafnium as framework cations. The phosphates reported in current work are colored in green-blue that significantly differs from the color of $K_2Mn_{0.5}Ti_{1.5}(PO_4)_3$ which is dark brown. As it could be assumed from the spectroscopic investigations, the reported compounds contain manganese (II) and manganese (III) at the same time. The oxidation of Mn^{2+} by air oxygen and stabilization of Mn^{3+} in the fluoride–phosphate flux can be explained by the anionic exchange between Mn^{2+} and $[M^{IV}F_6]^{2-}$ (MIV—Zr, Hf) ions with formation of $[Mn^{3+}F_6]^{3-}$ and $M^{IV}_x(PO_4)_y^{n-}$ ones (see Eqs. (1) and (2)). Under crystallization conditions $[Mn^{3+}F_6]^{3-}$ can dissociate and connect with $M^{IV}_x(PO_4)_y^{n-}$ forming the rigid langbeinite framework (Eq. (3)). Taking into account the presence of bivalent manganese in the flux $\{Mn_{0.5}M_{1.5}^{IV}(PO_4)_3^{2-}\}_m$ anion framework possibly originates (Eq. (4)), and as a result the obtained crystals will contain mixed-valent manganese. Thus, the presence of the large

Table 2
Atomic Coordinates and U_{eq} for $K_{1.96}Mn_{0.57}Zr_{1.43}(PO_4)_3$ and $K_{1.93}Mn_{0.53}Hf_{1.47}(PO_4)_3$ in $P2_13$

Atom	Site	Occ.	x	y	z	U_{eq}
$K_{1.96}Mn_{0.57}Ti_{1.43}(PO_4)_3$						
Zr1/Mn1	4a	0.742(17)/0.258(17)	0.14515(3)	0.14515(3)	0.14515(3)	0.0109(2)
Zr2/Mn2	4a	0.687(17)/0.313(17)	0.41477(4)	0.41477(4)	0.41477(4)	0.0107(2)
K1	4a	0.991(10)	0.70397(16)	0.70397(16)	0.70397(16)	0.0525(8)
K2	4a	0.968(10)	0.93081(13)	0.93081(13)	0.93081(13)	0.0425(7)
P1	12b	1	0.46204(9)	0.23155(9)	0.12613(9)	0.0116(2)
O1	12b	1	0.3194(3)	0.2344(3)	0.0813(3)	0.0248(7)
O2	12b	1	0.5476(3)	0.2964(4)	0.0226(3)	0.0287(7)
O3	12b	1	0.5059(3)	0.0907(3)	0.1497(4)	0.0283(7)
O4	12b	1	0.4802(4)	0.3085(4)	0.2511(3)	0.0339(9)
$K_{1.93}Mn_{0.53}Hf_{1.47}(PO_4)_3$						
Hf1/Mn1	4a	0.754(5)/0.246(5)	0.14479(2)	0.14479(2)	0.14479(2)	0.00819(10)
Hf2/Mn2	4a	0.716(5)/0.284(5)	0.41443(2)	0.41443(2)	0.41443(2)	0.00782(10)
K1	4a	0.972(9)	0.70444(15)	0.70444(15)	0.70444(15)	0.0478(8)
K2	4a	0.961(9)	0.93099(12)	0.93099(12)	0.93099(12)	0.0393(7)
P1	12b	1	0.46187(9)	0.23135(9)	0.12606(9)	0.0090(3)
O1	12b	1	0.3189(3)	0.2346(3)	0.0799(3)	0.0219(7)
O2	12b	1	0.5476(3)	0.2971(3)	0.0216(3)	0.0257(7)
O3	12b	1	0.5060(3)	0.0906(3)	0.1488(3)	0.0242(6)
O4	12b	1	0.4800(3)	0.3080(3)	0.2521(3)	0.0288(8)

amounts of fluoride in phosphates fluxes and at the same time formation of langbeinite-related phosphates gives the possibility to stabilize threevalent manganese.

3.2. Crystal structure

Both reported compounds crystallize in cubic system and are isotypic with the mineral langbeinite $K_2Mg_2(SO_4)_3$ [30]. The framework contains isolated $[MO_6]$ octahedra and $[PO_4]$ tetrahedra, which share their vertices (Fig. 1). Two nearest $[MO_6]$ octahedra are connected using three orthophosphate bridges into $[M_2P_3O_{18}]$ unit. Between two nearest units, which have common axis two positions of alkaline metal are located. Manganese and zirconium or hafnium atoms are six coordinated. Six vertices belonging to the same number of orthophosphate groups form oxygen environment of the network cation. M–O bond lengths are similar to both compounds and ranging from 2.069(3) to 2.102(3) for zirconium phosphate and from 2.051(3) to 2.102(3) Å for hafnium phosphate. Insignificantly small deviation of interatomic distances for corresponding bonds and cell parameters for both compounds can be explained by the fact that the value of effective ionic radius of zirconium (0.72 Å) just a little higher than for hafnium (0.71 Å) [31]. Bond valence calculations were performed for the oxygen environment of transition metal (for Mn bonding parameters were taken from [32], for Zr and Hf from [33]). The calculated values of BVS for Zr1 are equal to 4.02, for Zr2 are 3.975 and for Mn1 is 2.493, for Mn2 is 2.463 in zirconium compound. In $K_{1.93}Mn_{0.53}Hf_{1.47}(PO_4)_3$ the BVS is the next: 3.972, 3.927, 2.556 and 2.526 for Hf1, Hf2, Mn1 and Mn2 atoms, respectively. The values of BVS for manganese atoms in
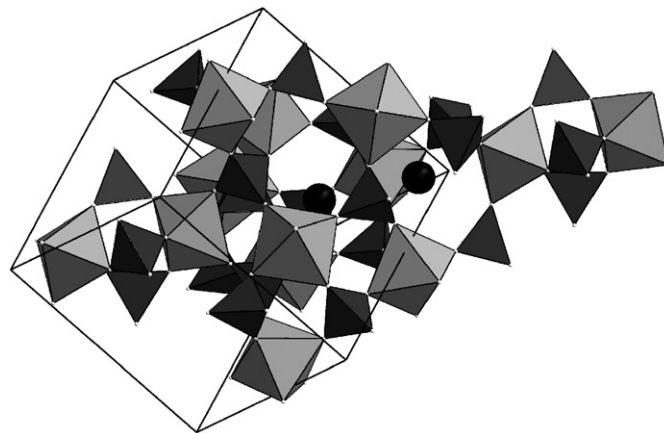

Fig. 1. Architecture of $\{M_2(PO_4)_3\}_\infty$ framework. $[MO_6]$ octahedra—light gray, $[PO_4]$ tetrahedra—dark gray, potassium cations—black circles.

both langbeinites are much higher than 2. Accordingly to the listed above values near the half of the manganese amount must be threevalent. The quantity of threevalent manganese calculated from the chemical composition much smaller than a half. The difference between the quantity of threevalent manganese in investigated compounds can be explained by the fact that experimental values of M–O bond lengths are superposition of Mn–O and Zr(Hf)–O ideal bonds which significantly differ one from another. Thus, the following chemical compositions of the reported phosphates should be assumed: $K_{1.96}Mn^{II}_{0.39}Mn^{III}_{0.18}Zr_{1.43}(PO_4)_3$ and $K_{1.93}Mn^{II}_{0.40}Mn^{III}_{0.13}Hf_{1.47}(PO_4)_3$.

The orthophosphate tetrahedra are close to regular. P–O bond lengths are characteristic for orthophosphate group [34] and O–P–O angles are close to tetrahedral. K1 atom has nine coordinated oxygen environment, while K2 has 12

Table 3
Selected Geometric parameters (Å, deg) for $K_{1.96}Mn_{0.57}Zr_{1.43}(PO_4)_3$ and $K_{1.93}Mn_{0.53}Hf_{1.47}(PO_4)_3$

	$K_{1.96}Mn_{0.57}Zr_{1.43}(PO_4)_3$	$K_{1.93}Mn_{0.53}Hf_{1.47}(PO_4)_3$
M1/Mn1–O1[i, ii]*	2.102(3) × 3	2.102(3) × 3
M1/Mn1–O2[iii, iv, v]*	2.069(3) × 3	2.051(3) × 3
M2/Mn2–O3[vi, vii, viii]*	2.078(3) × 3	2.073(3) × 3
M2/Mn2–O4[i, ii]*	2.101(3) × 3	2.087(3) × 3
P1–O1	1.527(3)	1.531(3)
P1–O2	1.523(3)	1.532(3)
P1–O3	1.525(3)	1.521(3)
P1–O4	1.510(3)	1.515(3)
K1–O1[vi, vii, viii]	2.939(4) × 3	2.923(4) × 3
K1–O2[ix, x, xi]	3.141(4) × 3	3.139(4) × 3
K1–O4[ix, x, xi]	3.263(4) × 3	3.254(4) × 3
K2–O3[ix, x, xi]	2.950(4) × 3	2.9535(17) × 3
K2–O2[xii, xiii, xiv]	3.067(4) × 3	3.053(4) × 3
K2–O4[ix, x, xi]	3.188(4) × 3	3.174(4) × 3
K2–O4[xii, xiii, xiv]	3.284(4) × 3	3.287(4) × 3
O1–P1–O2	109.31(19)	108.67(19)
O1–P1–O3	110.22(19)	110.39(18)
O1–P1–O4	111.1(2)	111.4(2)
O2–P1–O3	110.6(2)	110.47(19)
O2–P1–O4	106.8(2)	107.10(19)
O3–P1–O4	108.7(2)	108.7(2)

*M—Zr, Hf. Symmetry codes: (i) z, x, y; (ii) y, z, x; (iii) $-z, x-1/2, 1/2-y$; (iv) $1/2-y, -z, x-1/2$; (v) $x-1/2, 1/2-y, -z$; (vi) $1/2+y, 1/2-z, 1-x$; (vii) $1/2-z, 1-x, 1/2+y$; (viii) $1-x, 1/2+y, 1/2-z$; (ix) $1-y, 1/2+z, 3/2-x$; (x) $3/2-x, 1-y, 1/2+z$; (xi) $1/2+z, 3/2-x, 1-y$; (xii) $3/2-y, 1-z, 1/2+x$; (xiii) $1-z, 1/2+x, 3/2-y$; (xiv) $1/2+x, 3/2-y, 1-z$.

coordinated one. The values of K–O interatomic distances are close for both compounds. Selected geometric parameters are listed in Table 3.

3.3. FTIR-, UV–VIS- and EPR-spectroscopy

The FTIR-spectra of $K_{1.96}Mn_{0.57}Zr_{1.43}(PO_4)_3$ and $K_{1.93}Mn_{0.53}Hf_{1.47}(PO_4)_3$ are shown in Fig. 2. In general, both spectra are similar. Three groups of vibrations could be observed in a wavenumber region 400–1500 cm^{-1}. First group that includes P–O stretching frequencies is limited by 900 and 1200 cm^{-1}: strong single band at 1157 for $K_{1.96}Mn_{0.57}Zr_{1.43}(PO_4)_3$ (1160 for $K_{1.93}Mn_{0.53}Hf_{1.47}(PO_4)_3$); 1079 (1082) shoulder, 1036 (1046), 1016 (1016), 977 (985) and 914 (933) cm^{-1} shoulder. The second group of the bands contains bending vibrations of [PO$_4$] anion: three strong single peaks at 637 (638), 589 (590) and 554 (554) cm^{-1}. M–O vibrations could be observed in the third group. In spectrum of $K_{1.93}Mn_{0.53}Hf_{1.47}(PO_4)_3$ only two bands belonging to the latter subgroup are located at 442 and 418 cm^{-1}. Decoupling of those lines were found for $K_{1.96}Mn_{0.57}Zr_{1.43}(PO_4)_3$. Band at 442 is split into two bands at 445 and 436 cm^{-1}, band at 418 is split into two ones at 425 and 416 cm^{-1}.

Diffuse reflectance electron spectra of the titled compounds indicate the presence of manganese (III) in

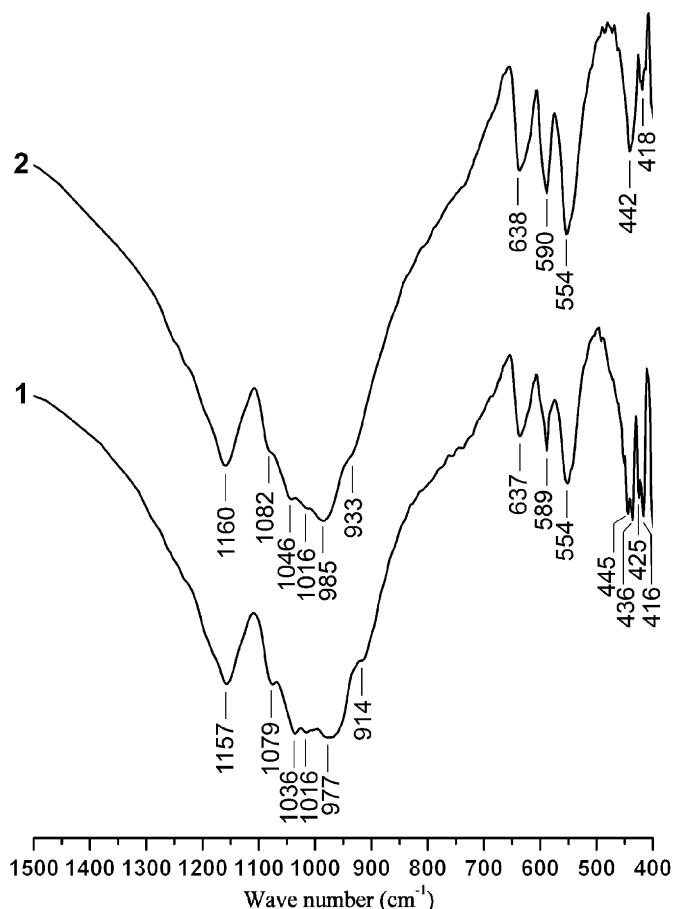Fig. 2. FTIR- spectra of (1) $K_{1.96}Mn_{0.57}Zr_{1.43}(PO_4)_3$ and (2) $K_{1.93}Mn_{0.53}Hf_{1.47}(PO_4)_3$.

obtained compounds (Fig. 3). The bands that correspond to the electron transition in Mn^{2+} (d^5 shell) were not found in presented spectra in a reason of their prohibition by spin (term ^6S). The bands observed in those spectra should be assigned as transitions in the shell of Mn^{3+} (d^4, term ^5D). Five bands were separated using the multi-peak fitting of the experimental curve. For both spectra, the wavenumbers of the obtained peaks are similar. Thus, we present the general assigning of the bands because the resolution of the spectrometer and curve character does not give us possibility to determine the peak position accurately.

The polyhedra, which describe oxygen environment of manganese atoms, have been suggested as slightly distorted octahedra on the basis of structure investigations. They are elongated in the direction of axis 3. At the same time, manganese atom shifts from the polyhedron center. The symmetry of the coordination sphere of manganese is reduced to C_{3v}. Assuming the latter fact an energy level diagram for d^4-ion in distorted octahedral environment has been proposed (Fig. 4). Double bands between 15,000 and 18,000 cm^{-1} in both spectra were decoupled on two Gauss peaks at 15,340 and 17,370 cm^{-1}. They belong to $^5E(^5E_g) \rightarrow {}^5A_1$ (v_1) and $^5E(^5E_g) \rightarrow {}^5E(^5T_{2g})$ (v_2) electron transitions in Mn^{3+}. The next three bands at 29,000,
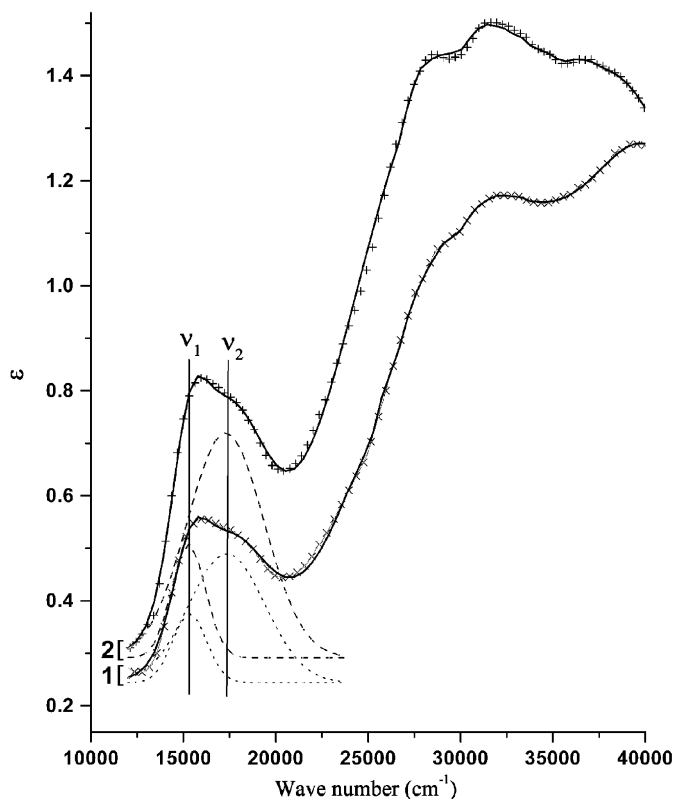
Fig. 3. UV–VIS diffuse reflectance electron spectra of (1) $K_{1.96}Mn_{0.57}Zr_{1.43}(PO_4)_3$ and (2) $K_{1.93}Mn_{0.53}Hf_{1.47}(PO_4)_3$. Solid line—fitted curve, + and × —collected spectra, dash and doted lines—gauss peaks.

Fig. 4. Splitting of the energy levels for d^4-ion in distorted octahedral environment.
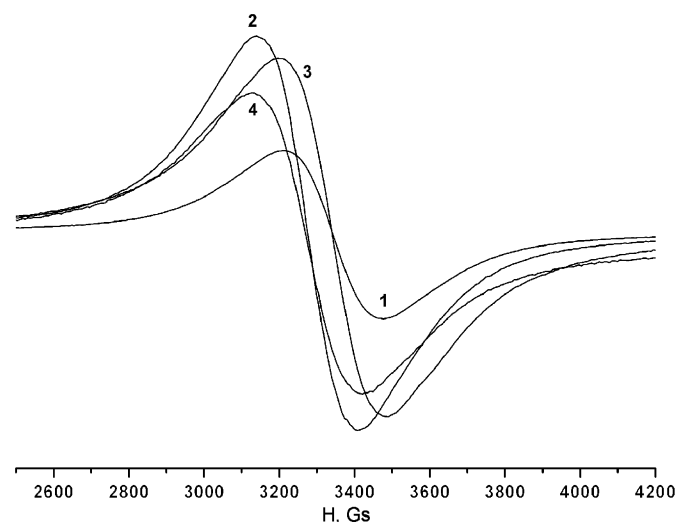
Fig. 5. EPR-spectra of $K_{1.96}Mn_{0.57}Zr_{1.43}(PO_4)_3$ (1–298, 2–77 K) and $K_{1.93}Mn_{0.53}Hf_{1.47}(PO_4)_3$ (3–298; 4–77 K).

33,850 and near 40,000 cm^{-1} should be assigned as charge transition bands from oxygen to manganese $O^{2-} \rightarrow Mn^{3+}$ [35].

Investigation of valent state of manganese in natural occurring minerals and their synthetic analogues andalusite ($Al_{2-x-y}Mn^{3+}_xFe^{3+}_yOSiO_4$) and henritermierite ($Ca_3Mn^{3+}_2(SiO_4)_2(OH)_4$) using the electron spectroscopy were reported earlier [36,37]. For the first compound were assumed tetragonal distorted oxygen environment of manganese (D_{4h}), while for the second were assumed axial distorted one (C_{2v}). Taking into account the symmetry of the environment three d–d transitions ($^5B_{1g} \rightarrow {}^5A_{1g}$; $^5B_{1g} \rightarrow {}^5B_{2g}$ and $^5B_{1g} \rightarrow {}^5E_g$ belonging Mn^{3+}) were found in spectra of andalousite and four ones assigned as $^5A_1 \rightarrow {}^5A_1$, $^5A_1 \rightarrow {}^5A_2$, $^5A_1 \rightarrow {}^5B_2$ and $^5A_1 \rightarrow {}^5B_1$ in henritermierite.

The EPR investigations were performed at 77 K and at room temperature (Fig. 5). In EPR spectra six bands are usually exist for Mn^{2+} (spin 5/2). At both temperatures in the collected spectra only one broad band ($\Delta H = 350\,Gs$) have been identified. For both compounds g-values are similar and are equal to 2.020 (298 K) and 2.017 (77 K). Large width of the band can be explained by the fact that manganese ions are not magnetically separated because of high occupancies of its positions, which are interlinked by orthophosphate groups. Similar broad band, which corresponds to Mn^{2+} was observed for γ-Mn_3O_4 previously [38].
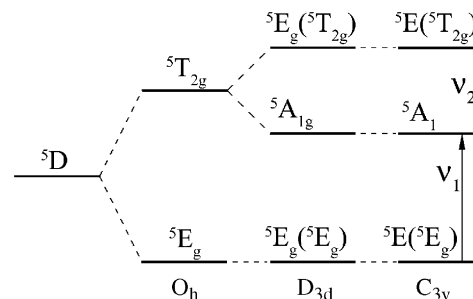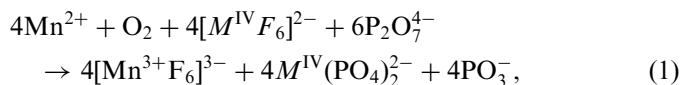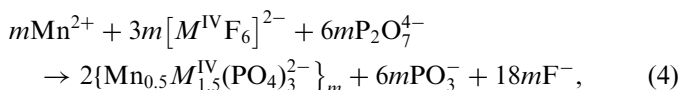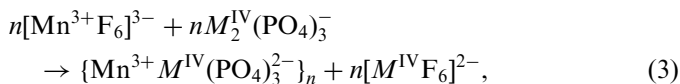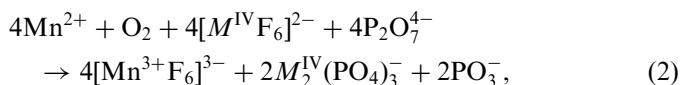
The values of g-factors are close to those for electron only. EPR- investigations prove the presence of Mn^{2+} in the obtained compounds. On the other hand, we cannot confirm the presence or absence of Mn^{4+} in the reported phosphates owing to the presence of mixed-valent system.

4. Conclusions

Complex phosphates containing Mn^{3+} can be synthesized by a high-temperature crystallization technique using the complex fluoride-containing phosphate flux on air. The quantity of threevalent manganese in the reported compounds varies from one third to one fourth from the total contents of the manganese. In the rigid langbeinite framework, manganese (II–III) and M(IV) are statistically distributed over two independent positions with similar octahedral oxygen environment. UV–VIS- and EPR-spectroscopy confirmed the presence of two different valent states of manganese in the obtained compounds.

$$4Mn^{2+} + O_2 + 4[M^{IV}F_6]^{2-} + 6P_2O_7^{4-}$$
$$\rightarrow 4[Mn^{3+}F_6]^{3-} + 4M^{IV}(PO_4)_2^{2-} + 4PO_3^-, \quad (1)$$

$$4Mn^{2+} + O_2 + 4[M^{IV}F_6]^{2-} + 4P_2O_7^{4-}$$
$$\rightarrow 4[Mn^{3+}F_6]^{3-} + 2M_2^{IV}(PO_4)_3^- + 2PO_3^-, \quad (2)$$

$$n[Mn^{3+}F_6]^{3-} + nM_2^{IV}(PO_4)_3^-$$
$$\rightarrow \{Mn^{3+}M^{IV}(PO_4)_3^{2-}\}_n + n[M^{IV}F_6]^{2-}, \quad (3)$$

$$mMn^{2+} + 3m[M^{IV}F_6]^{2-} + 6mP_2O_7^{4-}$$
$$\rightarrow 2\{Mn_{0.5}M_{1.5}^{IV}(PO_4)_3^{2-}\}_m + 6mPO_3^- + 18mF^-, \quad (4)$$

where M^{IV} = Zr, Hf.

References

[1] J.S. Stephens, C. Calvo, Can. J. Chem. 47 (1969) 2215–2225.
[2] E.V. Murashova, N.N. Chudinova, Russ. J. Inorg. Chem. 39 (1994) 1424–1429.
[3] K. Benkhouja, M. Zahir, A. Sadel, A. Handizi, A. Boukhari, E.M. Holt, J. Aride, M. Drillon, Mater. Res. Bull. 30 (1995) 49–55.
[4] Q. Huang, S.-J. Hwu, Inorg. Chem. 37 (1998) 5869–5874.
[5] P. Lightfoot, A.K. Cheetham, J. Chem. Soc. Dalton Trans. 89 (1989) 1765–1769.
[6] Y. Le Page, G. Donnay, Can. Mineral. 15 (1977) 518–521.
[7] P.B. Moore, Am. Mineral. 57 (1972) 1333–1344.
[8] E.C. Shafer, M.W. Shafer, R. Roy, Z. Kristallogr. 108 (1956) 263–275.
[9] M. Bagieu-Beucher, Acta Crystallogr. Sect. B 34 (1978) 1443–1446.
[10] A. Durif, M.T. Averbuch-Pouchot, Acta Crystallogr. Sect. B 38 (1982) 2883–2885.
[11] P. Lightfoot, A.K. Cheetham, A.W. Sleight, J. Solid State Chem. 73 (1988) 325–329.
[12] M.A.G. Aranda, J.P. Attfield, S. Bruque, Angew. Chem. Int. Ed. 31 (1992) 1090–1092.
[13] A.J. Wright, C. Ruiz-Valero, J.P. Attfield, J. Solid State Chem. 145 (1999) 479–483.
[14] A.J. Wright, J.P. Attfield, Inorg. Chem. 37 (1998) 3858–3861.
[15] E.V. Murashova, N.N. Chudinova, Crystallogr. Rep. 40 (1995) 476–484.
[16] E.V. Murashova, N.N. Chudinova, Crystallogr. Rep. 41 (1996) 845–850.
[17] R. Stief, C. Frommen, J. Pebler, W. Massa, Z. Anorg. Allg. Chem. 624 (1998) 461–468.
[18] C.O. Bjoerling, A. Westgren, Geol. Foeren. Stockholm Foerh. 60 (1938) 67–72.
[19] W. Eventoff, R. Martin, D.R. Peacor, Am. Mineral. 57 (1972) 45–51.
[20] O.V. Yakubovich, V.V. Bairakov, M.A. Simonov, Dokl. Akad. Nauk SSSR 307 (1989) 1119–1122.
[21] E.V. Murashova, N.N. Chudinova, Crystallogr. Rep. 41 (1996) 248–253.
[22] K.M.S. Etheredge, A.S. Gardberg, S.-J. Hwu, Inorg. Chem. 35 (1996) 6358–6361.
[23] I.V. Ogorodnyk, I.V. Zatovsky, V.N. Baumer, N.S. Slobodyanik, O.V. Shishkin, Acta Crystallogr. Sect. C 62 (2006) i100–i102.
[24] W.B. Blumenthal, The Chemical Behavior of Zirconium, Van Nostrand Co., New York, London, Toronto, 1958.
[25] V.A. Kopilevitch, L.N. Schegrov, A.F. Gafarova, N.H. Beckmetova, 1988, SU 1535821 A1 USSR.
[26] R.H. Blessing, Acta Crystallogr. Sect. A 51 (1995) 33–38.
[27] G.M. Sheldrick, SHELXS97 and SHELXL97. Program for Crystal Structure Solution and Refinement, University of Göttingen, Germany, 1997.
[28] I.V. Ogorodnyk, I.V. Zatovsky, N.S. Slobodyanik, V.N. Baumer, O.V. Shishkin, J. Solid State Chem. 179 (2006) 3461–3466.
[29] I.V. Ogorodnyk, I.V. Zatovsky, N.S. Slobodyanik, Russ. J. Inorg. Chem. 52 (2007) 121–125.
[30] A. Zemann, J. Zemann, Acta Crystallogr. 10 (1957) 409–413.
[31] R.D. Shannon, Acta Crystallogr. Sect. A 32 (1976) 751–767.
[32] I.D. Brown, D. Altermatt, Acta Crystallogr. Sect. B 41 (1985) 244–247.
[33] N.E. Brese, M. O'Keeffe, Acta Crystallogr. Sect. B 47 (1991) 192–197.
[34] D.E.C. Corbridge, second ed., Phosphorus. An Outline of its Chemistry, Biochemistry and Technology, vol. 2, Elsevier, Amsterdam, Oxford, New York, 1980.
[35] A.B.P. Lever, Inorganic Electronic Spectroscopy, second ed., Elsevier, Amsterdam, 1984.
[36] I. Abs-Wurmbach, K. Langer, E. Tillmanns, Naturwissenschaften 64 (1977) 527–528.
[37] U. Hålenius, Mineral. Mag. 68 (2004) 335–341.
[38] Z. Wu, K. Yu, Y. Huang, C. Pan, Y. Xie, Chem. Central J. 1 (2007) 1–8.